Role of Caspases, Bid, and p53 in the Apoptotic Response Triggered by Histone Deacetylase Inhibitors Trichostatin-A (TSA) and Suberoylanilide Hydroxamic Acid (SAHA)*

Clare Henderson‡§, Michela Mizzau‡§, Gabriela Paroni‡§¶, Roberta Maestro‖, Claudio Schneider‡, and Claudio Brancolini‡§‡‡**

*From the ‡Dipartimento di Scienze e Tecnologie Biomediche, Sezione di Biologia, Universita’ di Udine, P.le Kolbe 4, 33100 Udine Italy, **Laboratorio Nazionale Consorzio Interuniversitario Biotecnologie AREA Science Park, Padriciano 99 34142 Trieste Italy, ‖MMNP-Unit Experimental Oncology CRO-IRCCS National Cancer Institute Via Pedemontana Occ. 12 33081 Aviano (PN) Italy, and §MATI Center of Excellence, Universita’ di Udine. P.le Kolbe 4, 33100 Udine Italy*

Histone deacetylase activity is potently inhibited by hydroaximc acid derivatives such as suberoylanilide hydroxamic acid (SAHA) and trichostatin-A (TSA). These inhibitors specifically induce differentiation/apoptosis of transformed cells *in vitro* and suppress tumor growth *in vivo*. Because of its low toxicity, SAHA is currently evaluated in clinical trials for the treatment of cancer. SAHA and TSA induce apoptosis, which is characterized by mitochondrial stress, but so far, the critical elements of this apoptotic program remain poorly defined. To characterize in more detail this apoptotic program, we used human cell lines containing alterations in important elements of apoptotic response such as: p53, Bcl-2, caspase-9, and caspase-3. We demonstrate that caspase-9 is critical for apoptosis induced by SAHA and TSA and that efficient proteolytic activation of caspase-2, caspase-8, and caspase-7 strictly depends on caspase-9. Bcl-2 efficiently antagonizes cytochrome *c* release and apoptosis in response to both histone deacetylase inhibitors. We provide evidences that translocation into the mitochondria of the Bcl-2 family member Bid depends on caspase-9 and that this translocation is a late event during TSA-induced apoptosis. We also demonstrate that the susceptibility to TSA- and SAHA-induced cell death is regulated by p53.

Histone acetyl transferases and histone deacetylases (HDACs)[1] are emerging as important components that affect the dynamics of chromatin folding during gene transcription (1). HDACs catalyze the hydrolyisis of acetyl groups from ami-no-terminal lysine residues of the nucleosomal core histones (1, 2). Histone deacetylases inhibitors (HDIs) are promising agents for anticancer therapy; they exhibit strong antitumor activities *in vivo* with low toxicity in preclinical studies.

HADC inhibitors belong to a heterogenous class of compounds that includes derivatives of short chain fatty acids, hydroxamic acids, cyclic tetrapetides, and benzamides. Among the hydroxamic acids, trichostatin A (TSA) and suberoylanilide hydroxamic acid (SAHA) are commonly used inhibitors of HDACs (3, 4).

Numerous anti-proliferative effects have been reported for TSA and SAHA, including induction of G_0/G_2 cell cycle arrest, differentiation, and selective apoptosis of transformed cells (5–8). SAHA, in particular, shows strong anti-proliferative effects but low toxicity *in vivo* and is currently under clinical trials for the treatment of solid and hematological tumors (3, 4).

The cystein proteases, which belong to the family of caspases, play a critical role in the apoptotic response (9–11). Several anticancer drugs exert their antineoplastic activity by inducing tumor cell apoptosis. Various of these antitumor drugs trigger mitochondrial stress that can lead to apoptosome-mediated caspase-9 activation. Caspase-9 activates the effectors caspase-3 and -7, which then trigger cell fragmentation by cleaving selected death substrates and also process different caspases, thus leading to the generation of the amplification loop (12, 13).

An alternative apoptotic pathway is triggered by the cell surface death receptor (extrinsic pathway), which includes caspase-8 and caspase-10 as apical caspases (10, 11, 14). However by cleaving Bid, a Bcl-2 family member, these caspases can induce mitochondria permeabilization and activation of the amplifier function of the apoptosome (15).

Chemoresistance is frequently caused by aberrant apoptosis that in some instances has been related to defects in caspase activation (16, 17). Therefore, the definition of the apoptotic pathway that is induced by a particular anticancer drug is important to design therapeutic trials and clinical treatment.

The mechanism of HDI-induced apoptosis has only been marginally addressed. The role of the tumor suppressor p53 in the HDI-triggered apoptosis is not clear. Some reports have suggested an effect of p53 in this apoptotic response (18–21), whereas other studies have pointed to a p53-independent apoptotic response (22–24). Mitochondrial stress and release of cytochrome *c* mark the apoptotic response to HDIs (5, 23, 24, 26), and changes in the expression of Bcl-2 family members such as Bcl-2, Bax, or Bad have been detected in some cell lines

[1] The abbreviations used are: HDAC, histone deacetylase; WT, wild type; CI, catalytic-inactive; C3CI, caspase-3 catalytic inactive; C3WT, caspase-3 WT; C9DN, caspase-9 dominant negative; DNR, daunorubicin; ET-18-OCH₃, 1-*O*-octadecyl-2-*O*-methyl-sn-glycero-3-phosphocholine; HDI, histone deacetylase inhibitor; GFP, green fluorescent protein; p53DN, p53 dominant negative; PARP, polyADP-ribosyltransferase; SAHA, suberoylanilide hydroxamic acid; TSA, trichostatin-A; zVAD-fmk, z-Val-Ala-Asp-fluoromethylketone; NEO, neomycin; TRITC, tetramethylrhodamine isothiocyanate; CHAPS, 3-[(3-cholamidopropyl)dimethylammonio]-1-propanesulfonic acid; E1A, adenovirus early region 1A.

(26, 27). Caspase-3 activation was reported by different studies (5, 23, 24, 26), but cell death after SAHA treatment was observed also in the presence of pancaspase inhibitor zVAD-fmk (23). However, the same study suggested that a caspase not efficiently inhibited by zVAD-fmk could be involved in transducing the apoptotic signal triggered by SAHA (23).

Our work was designed to identify the critical elements involved in transducing HDI-induced apoptotic signals. Human cell lines containing known mutations in key elements of the apoptotic pathway allowed us to elucidate caspase-9 requirements in the apoptotic response to HDIs. We show that HDI-induced proteolytic activation of caspase-2, caspase-8, and caspase-7 was strictly dependent on caspase-9. Moreover, HDIs provoke, late during apoptosis, translocation of the Bcl-2 family member Bid into the mitochondria, and this translocation also depends on caspase-9. We also show that Bcl-2 efficiently antagonizes cytochrome *c* release and apoptosis in response to TSA. Finally, we demonstrate that the susceptibility to cell death in response to TSA and SAHA treatment is regulated by p53.

EXPERIMENTAL PROCEDURES

Culture Conditions and Drug Treatment—IMR90, IMR90-E1A, IMR90-E1A/C9DN (31) MCF-7/caspase-3 wt (C3WT), MCF-7/caspase-3 CI (C3CI), MCF-7/NEO, and MCF-7/C9DN were grown in Dulbecco's modified Eagle's medium supplemented with 10% fetal calf serum, penicillin (100 units/ml), glutamine (2 mM), and streptomycin (100 μg/ml) at 37 °C in 5% CO_2 atmosphere. Cells were cultured for 12–60 h with 1 μM TSA, for 24–48 h with 2.5 μM SAHA, for 44 h with 40 μM colchicine, for 44 h with 14 μM 1-*O*-octadecyl-2-*O*-methyl-sn-glycero-3-phosphocholine or for 44 h with 10 μM daunorubicin. Early passage BJ normal human foreskin fibroblasts were maintained in minimum essential medium with Earle's salts supplemented with non-essential amino acids and 10% fetal bovine serum (Invitrogen) at 37 °C in the presence of 5% CO_2.

In all trypan blue exclusion assays, 480–2400 cells, from three independent samples, were counted for each data point; data were calculated as the means of at least three independent experiments. The number of apoptotic cells (blue cells) was expressed as a percentage of the total cell number.

Transfection, Microinjection, and Time Lapse Analysis—For Bcl-2 survival activity, transfections were performed using the calcium phosphate precipitation method. Cells were seeded at 1.2×10^4 cell/ml, and after 18 h, they were co-transfected with 2 μg of Bcl-2 expression plasmid or NEO expression plasmid were together with 200 ng of p*EGFP-N1* (Invitrogen) to score the transfected cells *in vivo*. After 24 h, transfected cells were incubated with 1 μM TSA.

Microinjection was performed using the automated injection system (Zeiss, Germany) as described previously (28). Cells were injected with 10 ng of p*EGFPN1Bid* for 0.5 s at a constant pressure of 50 hPA. Time-lapse studies were performed using a laser scan microscopy Leica TCS-SP in a 5% CO_2 atmosphere at 37 °C. *In vivo* labeling of mitochondria with a MitoTracker (Molecular Probes) at a final concentration of 12.5 ng/ml was performed as described previously (29).

Retroviral Infection—BJ-E1A Ha-RasV12, BJ-E1A Ha-RasV12 MDM2, BJ-E1A Ha-RasV12 p53DN and BJ-E1A Ha-RasV12 Bcl-2 were generated as described previously (42). Briefly, pBABE-Puro Ha-rasV12, Wzl-Neo E1A 12S, pHygro-MaRXmdm2, pHygro-MaRX bcl2 WZLHygro DN p53 (175 H) were used to singularly transfect the amphotropic packaging cell line LinX-A (30). Transfection was performed by the calcium phosphate method. At 72 h after transfection, viral supernatants were collected, filtered, supplemented with 4 mg/ml polybrene, and combined to obtain the oncogene combinations described in the text to infect early passage BJ cells. After infection, cells were selected with a combination of hygromycin (50 μg/ml), puromycin (1 μg/ml), and neomycin (300 μg/ml) for 7 days. Effective infection was confirmed by Western blot analysis.

Cell Fractionation and Western Blotting—In all the experiments presented, cell lysates were prepared from floating death cells and adherent cells harvested together. For subcellular fractionation with the Dounce homogenizer, after washing, cells were resuspended in extraction buffer B (20 mM Hepes, pH 7.5, 1.5 mM $MgCl_2$, 1 mM EDTA, 1 mM EGTA, 1 mM dithiothreitol, 250 mM saccarose, 10 μg/ml cytocha-

lasin B, 1 mM dithiothreitol, 1 mM phenylmethylsulfonyl fluoride, and 10 μg/ml each of chymostatin, leupeptin, antipain, and pepstatin), incubated for 20 min on ice, and then subjected to 40 strokes in a glass Dounce homogenizer type B. The obtained cell lysate was centrifuged twice at $13,500 \times g$ for 10 min. The obtained pellet was considered as crude mitochondrial fraction, and the supernatant was considered as crude cytosolic fraction.

For Western blotting, proteins were transferred to a 0.2-μm pore-sized nitro-cellulose membrane (Schleicher & Schuell) using a semidry blotting apparatus (transfer buffer: 20% methanol, 48 mM Tris, 39 mM glycine, and 0.0375% SDS). After staining with Ponceau S, the nitro-cellulose sheets were saturated for 1 h in Blotto-Tween 20 (50 mM Tris-HCl, pH 7.5, 200 mM NaCl 5% non-fat dry milk, and 0.1% Tween 20) and incubated overnight at room temperature with the anti-caspase-2 (31), anti-caspase-8 (Alexis), anti-caspase-7 (Cell Signaling), anti-calnexin (Transduction Laboratories), anti-p85 polyADP-ribosyltransferase (PARP) fragment (Promega), anti-cytochrome *c* (Transduction Laboratories) anti-tubulin, anti-Bid (Cell Signaling). Blots were then rinsed three times with Blotto-Tween 20 and incubated with peroxidase-conjugated goat anti-rabbit (KPL) or goat anti-mouse (Euroclone) for 1 h at room temperature. Blots were then washed three times in Blotto-Tween 20, rinsed in phosphate-buffered saline and developed with Super Signal West Pico, as recommended by the vendor (Pierce).

Immunofluorescence Microscopy—For indirect immunofluorescence microscopy, cells were fixed with 3% paraformaldehyde in phosphate-buffered saline for 20 min at room temperature. Fixed cells were washed with phosphate-buffered saline/0.1 M glycine, pH 7.5, and then permeabilized with 0.1% Triton-X100 in phosphate-buffered saline for 5 min. The coverslips were treated with the anti-cytochrome *c* antibody (Promega), diluted in phosphate-buffered saline, for 45 min in a moist chamber at 37 °C. They were then washed with n twice and incubated with the relative TRITC-conjugated secondary antibodies (Sigma) for 30 min at 37 °C. Cells were examined with a laser scan microscope (Leica TCS NT) equipped with a 488–534 λ argon laser and a 633 λ helium-neon laser.

In Vitro Proteolytic Assay—Caspase-3 was expressed in bacteria and purified as described previously (31) using the pQE-12 expression system (Qiagen). Caspase-2 lacking the prodomain, caspase-2Δ-1–152, was expressed as glutathione *S*-transferase fusion protein in bacteria. The activity of purified recombinant caspase-2 was monitored by measuring the K_m values toward the pentapeptide Ac-VDVAD-pNA (32). Assays of chromogenic substrate cleavage contained 50 mM Hepes, pH 7.2, 50 mM NaCl, 0.1% CHAPS, 10 mM EDTA, pH 8.0, 5% glycerol, 10 mM dithiothreitol. Enzyme-catalyzed release of *p*-nitroanilide was monitored at 405 nm in a microtiter plate reader (Bio-Tek).

Caspase-2 was *in vitro* translated with ^{35}S label using the TNT-coupled reticulocyte lysate system (Promega). 1 μl of *in vitro* translated caspase-2 was incubated with increasing amounts of recombinant caspase-3 or caspase-2 in 15 μl of the appropriate buffer (final volume) for 1 h at 37 °C. Reactions were terminated by adding one volume of SDS gel loading buffer and boiling for 3 min.

RESULTS

Characterization of the Apoptotic Response to TSA in MCF-7 and MCF-7 Caspase-3 Cells—To characterize the apoptotic response triggered by TSA, we used MCF-7, a cell line that does not express caspase-3 activity (31). For comparison, MCF-7 was rescued for caspase-3 either with C3WT or with its catalytically inactive form, C3CI. These cell lines were grown in the presence of 1 μM TSA for 44 h. To compare the proapoptotic effect of TSA, the same cell lines were incubated with well characterized death triggers as indicated (Fig. 1*a*). TSA efficiently induced apoptosis in MCF-7/C3WT cells with ~80% of cell death after 44 h of treatment. In MCF-7/C3CI, the apoptotic response was reduced to 20%, thus suggesting a critical role for caspase-3. The same experimental system was probed with other known apoptotic inducers. The microtubule-disrupting compound colchicine showed only a weak induction of apoptosis with ~20% of cells having apoptotic features. Treatment with daunorubicin (DNR), which induces genotoxic stress (33), caused cell death in ~50% of the cells, and again, this apoptotic response was reduced in the absence of active caspase-3. We also evaluated the apoptotic effect of the ether lipid 1-*O*-octa-
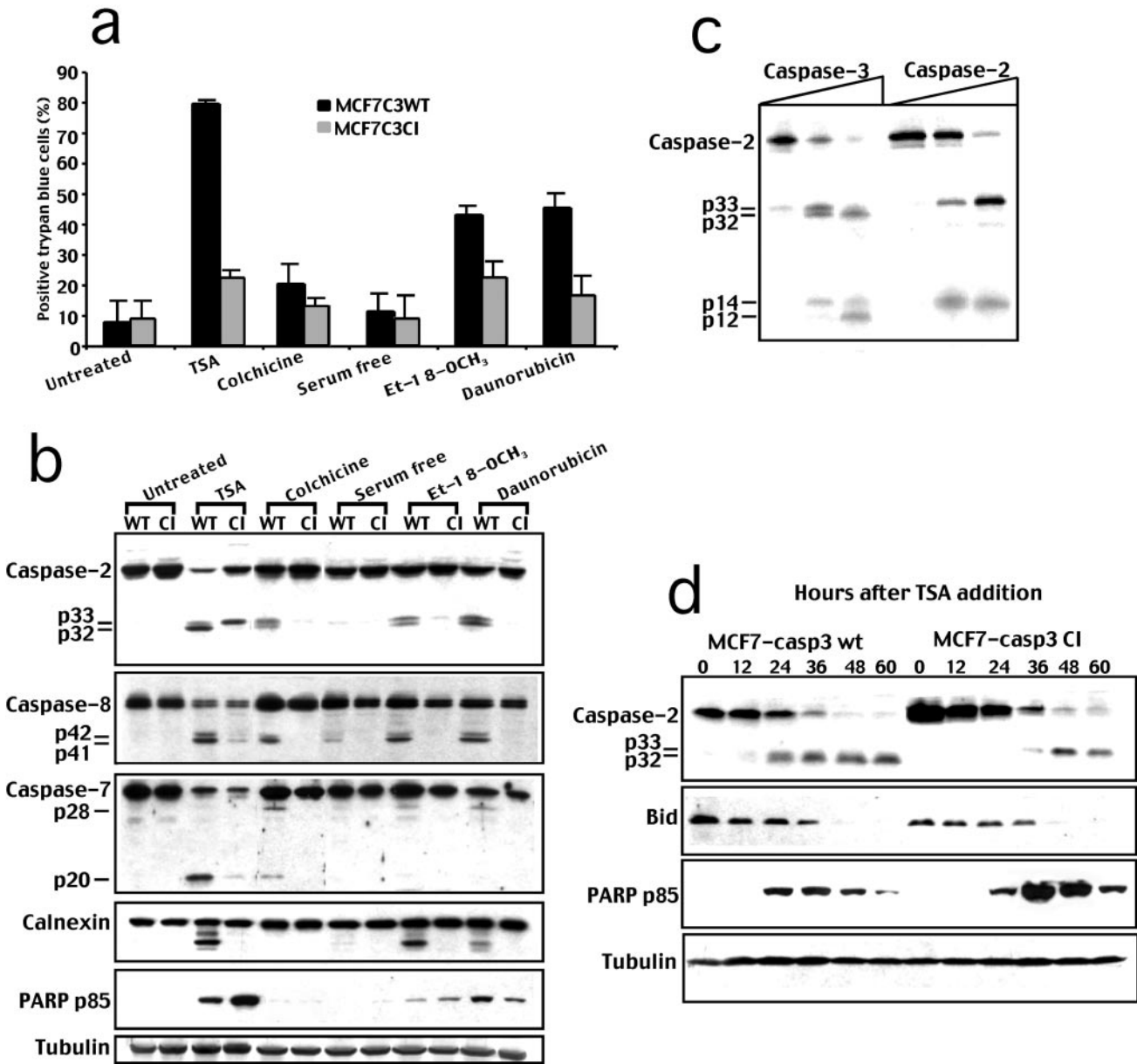
FIG. 1. **TSA-induced caspases processing and apoptotic cell death in MCF-7/C3WT and MCF-7/C3CI cells.** As shown in *a*, MCF-7/C3WT and MCF-7/C3CI cells were treated with the indicated apoptotic stimuli, and the appearance of apoptosis was scored with trypan blue staining as indicated under "Experimental Procedures." *b*, processing of caspases in MCF-7/C3WT and MCF-7/C3CI cells treated with different apoptotic insults. Equal amounts of MCF-7/C3WT and MCF-7/C3CI cell lysates were subjected to SDS-PAGE electrophoresis. Immunoblots were performed using the indicated antibody. *c, in vitro* proteolytic processing of caspase-2. [^{35}S]methionine-labeled *in vitro* translated caspase-2 was incubated for 1 h at 37 °C with increasing amounts of recombinant caspase-2 and caspase-3. *d*, time course analysis of caspase-2, Bid, and PARP processing in MCF-7/C3WT and MCF-7/C3CI cells treated with TSA. Equal amounts of MCF-7/C3WT and MCF-7/C3CI cell lysates at the different time points were subjected to SDS-PAGE electrophoresis. Immunoblots were performed using the indicated antibody.

decyl-2-*O*-methyl-sn-glycero-3-phosphocholine (ET-18-OCH₃) (34). Apoptosis was induced by the ether lipid in more than 50% of the MCF-7/C3WT cells, and this response was reduced in MCF-7/C3CI cells. In the absence of serum, no significant levels of cell death could be detected.

Processing of caspase-2, -7, and -8 in response to the different apoptotic triggers was next investigated by immunoblotting. In MCF-7/C3WT cells that were treated with colchicine, ET-18-OCH₃, and DNR, caspase-2 typically resulted in processed products migrating as a doublet at 33 and 32 kDa, respectively (Fig. 1*b*). On the contrary, similar treatments in MCF-7/C3CI cells resulted in lower amounts of processed caspase-2 products, thus indicating that caspase-3 is strictly

required for the observed processing. TSA treatment induced a strong processing of caspase-2 but, in contrast to the results with other proapoptotic agents, significant caspase-2 processing was also detectable in MCF-7/C3CI cells. Interestingly, although in MCF-7/C3WT cells, caspase-2 processing could be detected as p33 and p32 cleaved forms, in MCF-7/C3CI cells, only the p33 product was detected. To confirm that the generation of the p33 and p32 forms of caspase-2 could result from the proteolytic activity of different caspases, *in vitro* protelytic assays using recombinant caspase-2 and caspase-3 were performed. As shown in Fig. 1*c*, recombinant caspase-3 processed caspase-2 and generated both the p33 and the p32 forms, whereas when caspase-2 was processed by itself (re-

HDIs and Cell Death

combinant caspase-2), only the p33 form was observed.

In MCF-7/C3WT cells, TSA, colchicine, ET-18-OCH$_3$, and DNR induced activation of caspase-8, as detected by the appearance of the processed p42/41 intermediate fragments (Fig. 1*b*). In MCF-7/C3CI cells, activation of caspase-8 was barely detectable in response to colchicine, ET-18-OCH$_3$, and DNR. TSA treatment in the MCF-7/C3CI cells produced a clear decrease of the pro-caspase-8 as also observed for MCF-7/C3WT cells; however, only low amounts of the p42/41 fragments can be detected in absence of caspase-3 activity.

Caspase-7 was also processed into the typical p20 fragment in response to TSA, colchicine, ET-18-OCH$_3$, and DNR in MCF-7/C3WT cells. In MCF-7/C3CI cells, similarly to caspase-8, TSA induces a clear decrease in pro-caspase-7, but the amount of the p20 processing products was strongly reduced.

The same extracts were also probed for calnexin, a caspase-3-dependent substrate and PARP that exhibits caspase-3-independent processing (35). Whereas calnexin shows a caspase-3-dependent cleavage in the presence of TSA, the processed p85 PARP fragment was clearly observed in both MCF-7/C3WT and C3CI cells treated with ET-18-OCH$_3$, DNR, and TSA (Fig. 1*b*).

A time course analysis was performed to analyze, in more detail, caspase-2 processing in response to TSA and to investigate the caspase-3-independent cleavage of caspase-2. As shown in Fig. 1*d*, after addition of TSA, caspase-2 processing was readily detected after 24 h in MCF-7/C3WT cells. In contrast, in the caspase-3 mutant MCF-7/C3CI cells, processing of the p33 fragment was detected, only about 12 h later than in MCF-7/C3WT. It is noteworthy that PARP processing was increased in MCF-7/C3CI cells with respect to MCF-7/C3WT cells. We also investigated the processing of the BH3-only Bcl-2 family member Bid (15). As shown in Fig. 1*d*, Bid processing, detected as loss of the p22 kDa non-cleaved Bid version, was induced by TSA, but the similar results observed in MCF-7/C3CI and in MCF-7/C3WT cells indicated that this cleavage was caspase-3-independent.

Caspase-9 Is Required for Cell Death, Caspase-2, -7, and -8 Activation, and PARP Processing in Response to TSA—To further study the mechanism by which TSA induces apoptosis, we used MCF-7 cells expressing a dominant negative mutant form of caspase-9, MCF-7/C9DN (36). This mutant prevents the activation of caspase-9 but not the preceding steps of apoptosis by competing with endogenous caspase-9 for binding to APAF-1 (37).

Treatment of control MCF-7/NEO cells with TSA induced cell death in ~20 and ~35% of cells after 48 and 60 h, respectively. Cell death was clearly reduced in MCF-7/C9DN cells with residual 5% of death cells after 48 h and 10% of death cells after 60 h of TSA (Fig. 2*a*).

As shown in Fig. 2*b*, processing of caspase-2, -7, -8, and PARP in response to TSA treatment was strictly dependent on caspase-9. In fact, cleavage of caspase-2, -7, and -8 was undetectable in MCF-7/C9DN cells analyzed after 24 or 48 h of TSA treatment, whereas caspase-2 p33 processing, caspase-8 p42/p41 processing, caspase-7 p20 processing, and PARP p85 fragment were readily observed in the MCF-7/NEO cells.

To confirm the critical role of caspase-9 during TSA-induced cell death, a different caspase-9 defective cell line was analyzed. TSA sensitivity of IMR90 fibroblasts stably co-expressing the E1A oncogene together with a dominant negative form of caspase-9 IMR90-E1A/C9DN was compared with that of parental IMR90 cells expressing E1A alone. TSA response was also mediated by caspase 9 in IMR90-E1A fibroblasts (Fig. 2*c*), and as observed in MCF-7/C9DN cells, no processing of caspase-2, -7, -8, and PARP was detected in IMR90-E1A/C9DN fibroblasts after TSA treatment (Fig. 2*d*).

Bcl-2 Inhibits TSA-mediated Cytochrome c Release and Apoptosis—During stress-induced apoptosis, cytochrome *c* released from mitochondria binds to Apaf-1, and this promotes apoptosome formation and subsequent caspase-9 activation (9, 12). Having demonstrated that caspase-9 is required to transduce the apoptotic signal triggered by TSA, we next investigated whether TSA promotes cytochrome *c* release from the mitochondria. As shown in Fig. 3*a*, cytochrome *c* can be detected in the cytosolic fraction of MCF-7/NEO cells cultured for 36 h in the presence of TSA, and it was not present in the cytosolic fraction of untreated MCF-7/NEO cells. Cytochrome *c* localization was also analyzed by immunofluorescence. As shown in Fig. 3*b*, TSA treatment causes alterations in mitochondrial morphology and redistribution of cytochrome *c* in the cytoplasm.

On the whole, our data support the notion that TSA induces cytochrome *c* release that in turn leads to a caspase-9-dependent apoptosis. We next wanted to evaluate the effect of Bcl-2 on TSA-mediated cell death. Previous studies suggested that Bcl-2 can inhibit cytochrome *c* release and subsequent apoptosis in cells that were treated with HDIs (22, 23). Consistently, we observed that Bcl-2 overexpression inhibited TSA-mediated cell death in IMR90-E1A/NEO cells (Fig. 3*c*). Since Bcl-2 also antagonized cytochrome *c* release in IMR90-E1A/C9DN cells (Fig. 3*d*), we can conclude that Bcl-2 inhibition is upstream of caspase-9. Under the same conditions, placental alkaline phosphatase (PLAP), used as a control, was unable to block cytochrome *c* release from the mitochondria.

E1A Increases Susceptibility to SAHA- and TSA-induced Apoptosis—Different studies indicate that HDIs show selective toxicity for cancer cells (3, 4). We analyzed the apoptotic response to TSA and SAHA in primary IMR90 human fibroblasts as compared with IMR90 cells expressing the E1A oncogene. As an additional control, IMR90 co-expressing E1A and caspase-9 DN were employed. As revealed by the trypan blue exclusion assays, SAHA and TSA efficiently induced cell death in IMR90-E1A/NEO cells, whereas IMR90 parental cells showed a reduced sensitivity to HDI-induced cell death (Fig. 4*a*), thus supporting the notion of a differential sensitivity of transformed cells to HDIs. The critical role of caspase-9 in HDI-induced cell death was further supported by the observation of an impaired SAHA-induced apoptotic response in IMR90-E1A cells following expression of DN caspase-9.

Consistently, caspase-2 and PARP processing in response to TSA or SAHA was observed only in IMR90 cells expressing E1A but not in primary IMR90 fibroblasts. Of note, E1A expression in IMR90 fibroblasts resulted in significant higher caspase-2 levels. It has been recently shown that E1A can coordinate the up-regulation of multiple caspases, probably as a consequence of an unrestrained E2F activity (38). Thus changes in caspases levels are likely to contribute to the increased apoptotic susceptibility observed in E1A transformed cells.

Bid Processing and Translocation to the Mitochondria Require Caspase-9 Activity—Bid is a proapoptotic member of the Bcl-2 family of proteins that contains only a BH3 domain (15). Bid is a caspase-8 substrate that, once processed, translocates to the mitochondria and potently induces cytochrome *c* release. It has been reported that Bid processing in SAHA-treated CEM cells occurs even in the presence of the pancaspase inhibitor zVAD-fmk (23). We observed that Bid processing was detectable also in absence of caspase-3 (Fig. 1*c*); therefore, we wanted to investigate whether caspase-9 was required for Bid cleavage in response to HDIs. Immunoblotting analysis showed that during TSA- or SAHA-induced apoptosis, caspase-9 was required to induce Bid processing, as revealed by the disappear-
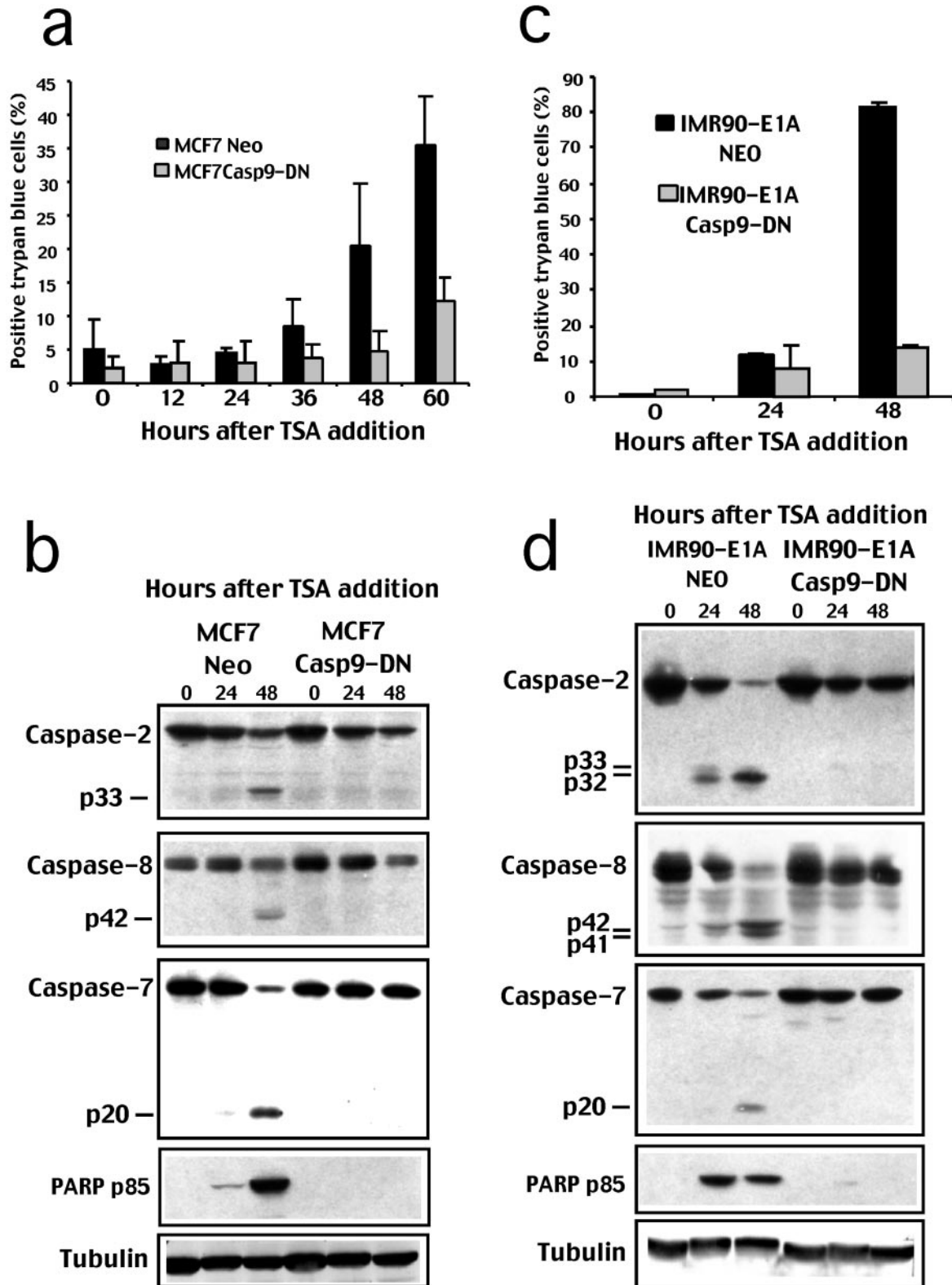
FIG. 2. **TSA-induced caspases processing and cell death require caspase-9.** As shown in *a*, MCF-7/Casp9-DN and MCF-7/NEO cells, as indicated, were treated with TSA for the indicated time points, and the appearance of apoptosis was scored by trypan blue staining as indicated under "Experimental Procedures." *b*, processing of caspases in MCF-7/Casp9-DN and MCF-7/NEO cells grown for the indicated time in the presence of TSA. Equal amounts of MCF-7/C3WT and MCF-7/C3CI cell lysates were subjected to SDS-PAGE electrophoresis. Immunoblots were performed using the indicated antibodies. As shown in *c*, IMR90-EIA/Casp9-DN and IMR90-E1A/NEO cells were treated with TSA for the indicated time points, and the appearance of apoptosis was scored with trypan blue staining as indicated under "Experimental Procedures." *d*, processing of caspases in IMR90-E1A/Casp9-DN and IMR90-E1A/NEO cells grown for the indicated time in the presence of TSA. Equal amounts of IMR90-E1A/Casp9-DN and IMR90-E1A/NEO cell lysates were subjected to SDS-PAGE electrophoresis. Immunoblots were performed using the indicated antibodies.

a

Hours after TSA addition

MCF7 Neo

b

c

d

FIG. 3. **TSA-induced cell death triggers cytochrome *c* (*Cyt. c*) release from mitochondria, which is counteracted by Bcl-2.** *a*, release of cytochrome *c* from mitochondria in cells treated with TSA. Crude mitochondrial (*P*) and cytosolic (*C*) fractions were obtained from MCF-7/NEO cells using Dounce homogenizer as described under "Experimental Procedures." Protein samples were prepared for Western blotting, and membranes were probed with the anti-cytochrome *c* antibody. As shown in *b*, MCF-7/NEO cells were treated or not (*untreated*) with TSA, and after 36 h, immunofluorescence assays were performed using anti-cytochrome *c* antibody. As shown in *c*, IMR90-E1A/NEO cells were co-transfected with the indicated constructs and pEGFP-N1 as a reporter. The appearance of the apoptotic cells was scored after 20 h from transfection. Cells showing a collapsed morphology and presenting extensive membrane blebbing were scored as apoptotic. Data represent arithmetic means ± S.D. of four independent experiments. As shown in *d*, IMR90-E1A/Casp-9 DN cells were co-transfected with the indicated constructs and pEGFP-N1 as a reporter. After the indicated times, from TSA treatment, cells were fixed, and an immunofluorescence assay was performed using anti-cytochrome *c* antibody. Cells co-expressing GFP and Bcl-2 or GFP and human placental alkaline phosphatase were scored for cytochrome *c* release from mitochondria. Data represent arithmetic means ± S.D. of three independent experiments.
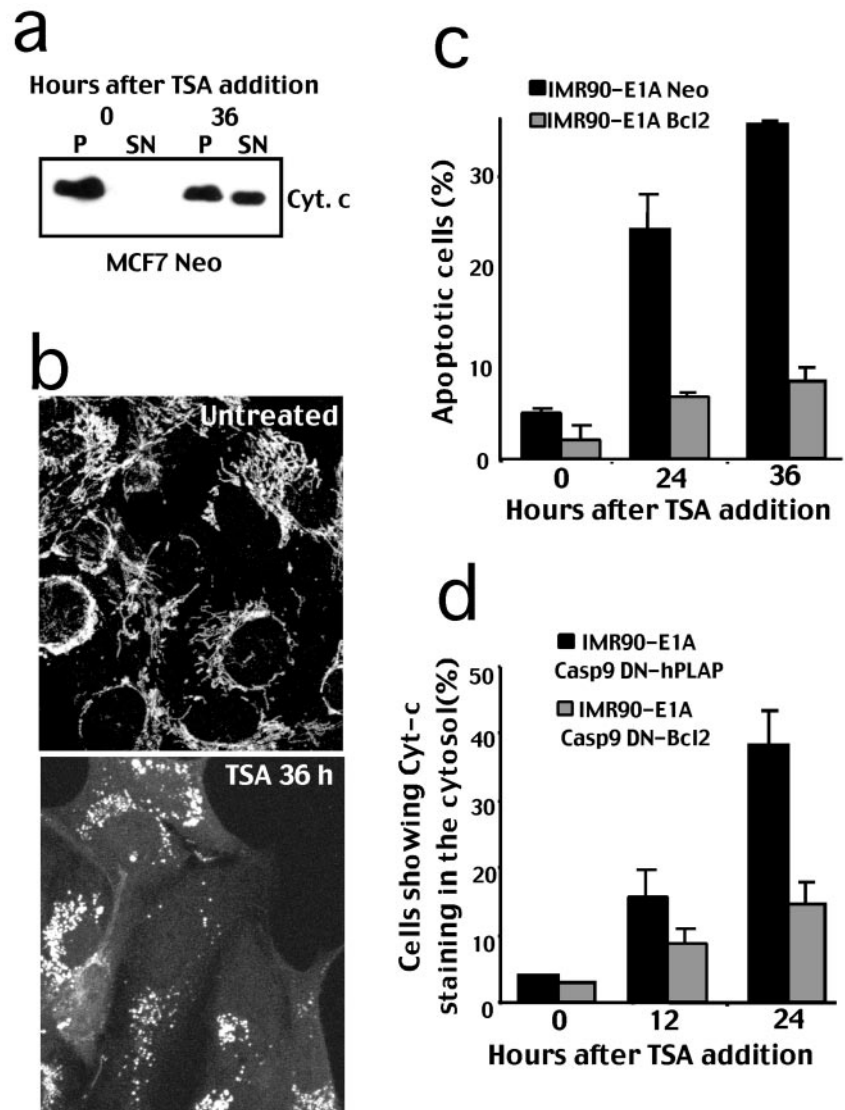
ance of the uncleaved Bid product (Fig. 5*a*). Again, caspase-2 processing was strictly correlated to caspase-9 activity. Tubulin was used as loading control.

Translocation of Bid to the mitochondria was then analyzed *in vivo* by time-lapse analysis. Time lapse assays allow analysis on a single cell basis followed in real time, and the timely appearance of cellular shrinkage/blebbing in relation to Bid-GFP translocation to the mitochondria could be monitored. The analysis was performed in both IMR90-E1A/NEO and IMR90-E1A/C9DN cells. As indicated in Fig. 5*b*, cells were incubated for 22 h with TSA and then microinjected with pEGFP-N1-*Bid* plasmid. 2 h after injection, cells were incubated with mitotracker (29) to visualize mitochondria, and time frames were collected every 5 min for 24 h. Selected frames of representative experiments at the indicated times are shown in Fig. 5*c*. Bid-GFP was initially detected as a diffuse signal throughout the cell body. In IMR90-E1A/NEO cells, TSA induced cell retraction, leading to cell collapse as early as 4.30 h after microinjection, whereas the translocation of Bid-GFP to the mitochondria was detectable only later (Fig. 5*c*, *arrowheads*). Neither cell collapsing, blebbing, nor translocation of Bid-GFP to the mitochondria could be detected in untreated cells under the same time course conditions (data not shown). Consistent with the results presented above in IMR90-E1A-expressing caspase-9 DN cells, TSA was unable to induce cell death under

the same time frame, and Bid-GFP was still detected as diffuse staining throughout the cell body as late as 21 h from microinjection. Histograms presented (Fig. 5*d*) summarize the results obtained from various experiments where each position along the *x* axis represents a single cell.

The Apoptotic Susceptibility to TSA and SAHA Is Dependent on p53—p53 tumor suppressor is the most mutated gene in cancer cells, and it regulates cell cycle arrest or apoptosis in response to pathological insults such as DNA damage or expression of mitogenic oncogenes (39, 40). As a consequence, inactivation of p53 can promote oncogenic transformation and resistance to many anticancer treatments (41). Thus defining the role of p53 during HDI-triggered apoptotic response is key for an optimal use of these drugs in clinics. Previous works have attempted to address this issue by using human cancer cell lines differing in the presence/absence of p53 gene alterations (22–24). It is clear that since cancer cell lines may have accumulated numerous additional genetic alterations, interpretation of the results is often difficult. Taking into account these caveats, we sought to investigate the role of p53 in HDIs apoptotic response by using human primary cells containing defined mutations affecting p53 function. For this purpose, early passage normal human foreskin fibroblasts (BJ) were transduced with E1A and Ha-RasV12 oncogenes by retroviral infection. To selectively knock-down p53 function, these cells

FIG. 4. **E1A increases susceptibility to SAHA- and TSA-induced apoptosis.** As shown in *a*, IMR90, IMR90-E1A/NEO, and IMR90-EIA/Casp9-DN cells were treated with TSA or SAHA for the indicated time points, and the appearance of apoptosis was scored with trypan blue staining as indicated under "Experimental Procedures." *b* and *c*, processing of caspases in IMR90, IMR90-E1A/NEO, and IMR90-EIA/Casp9-DN cells grown for the indicated time in the presence of TSA (*b*) or SAHA (*c*). Equal amounts of IMR90, IMR90-E1A/NEO, and IMR90-EIA/Casp9-DN cell lysates were subjected to SDS-PAGE electrophoresis. Immunoblots were performed using the indicated antibodies.
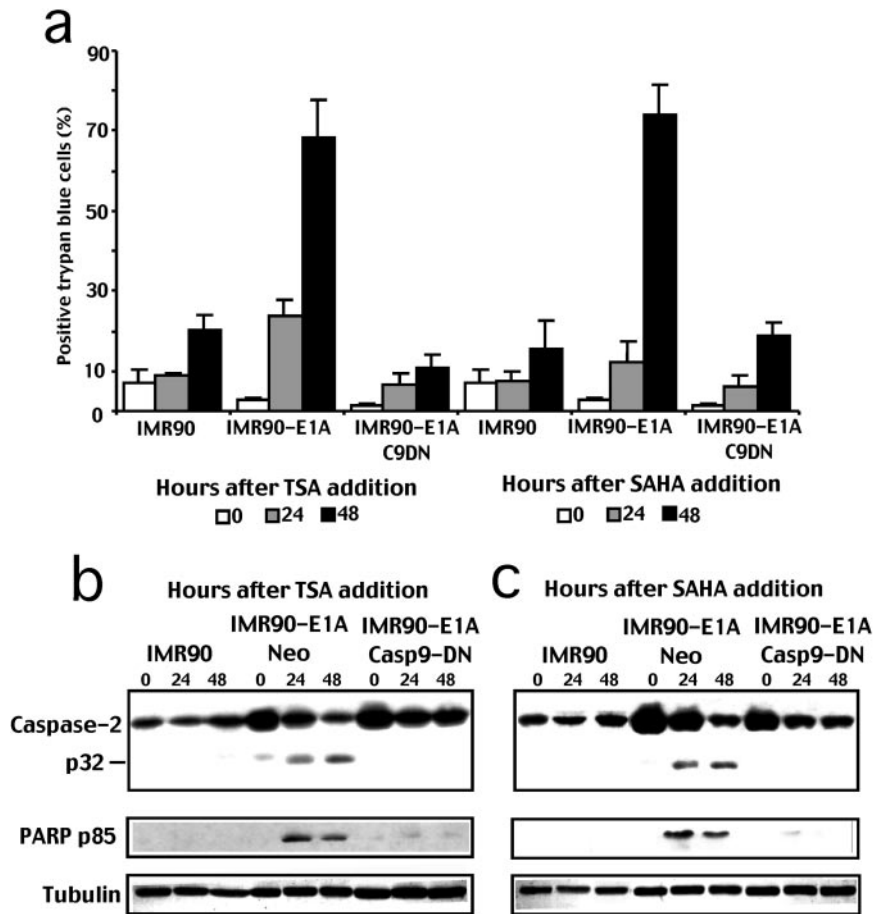
were further infected with retrovirus that drive the expression of either MDM2 or a dominant negative form of p53 (42). As a control, BJ-E1A/Ras cells were also infected with a retrovirus encoding Bcl-2.

The trypan blue assays (Fig. 6*a*) show that after 24 h of treatment with TSA or SAHA, BJ-E1A/Ras cells expressing MDM2 or p53DN were more resistant to cell death when compared with parental BJ-E1A/Ras with functional p53. When the same analysis was performed after 48 h from treatment, cells grown in the presence of SAHA and lacking functional p53 were still partially resistant to cell death, whereas cells treated with TSA were almost all dead, independently from the p53 status. Bcl-2 efficiently counteracted TSA and SAHA-induced apoptosis at both 24 and 48 h of treatment.

To confirm the role of p53 in the apoptotic response triggered by TSA and SAHA, immunoblotting. with antibodies specific for caspase-2, Bid, and tubulin was performed. Curiously, the p33 form of caspase-2 was already observed in untreated BJ cells (Fig. 6*b*). It is unlikely that this cleaved form is a consequence of a low level of cell death since PARP processing was undetectable under the same conditions (data not shown). Alternatively, it could be possible that in these cell lines, limited proteolytic processing of caspase-2 could occur independently from cell death or that this cleavage is a post-lysis processing.

As illustrated in Fig. 6*b*, the kinetics of caspase-2 and Bid processing in BJ-E1A/Ras expressing MDM2, p53DN, or Bcl-2 treated with TSA and SAHA was in accord with the trypan blue assays. The effect of p53 was particularly evident in cells treated with SAHA. Even after 48 h of SAHA treatment, a large amount of uncleaved caspase-2 and Bid could still be detected in MDM2- and p53DN-expressing cells, whereas the same death substrates were almost completely cleaved in BJ-E1A/Ras parental cells.

As mentioned previously, long term TSA treatment can induce cell death also independently from p53, and accordingly, caspase-2 and Bid proteolytic processing was almost complete, also in cells containing p53DN or MDM2. However, a shorter TSA treatment (24 h) left a larger amount of uncleaved caspase-2 and Bid in cells in which p53 was functionally inactivated with respect to WT p53 parental cells. Interestingly, acetylation of the histone H3 was more pronounced in cells treated with TSA respect to SAHA (Fig. 6*b*). It is well known that TSA is an inhibitor of HDACs at nanomolar range, whereas SAHA is efficient at micromolar range (3). Thus the difference in terms of apoptosis in cells treated with TSA and SAHA might reflect the potency of the two HDIs.

DISCUSSION

The definition of the apoptotic pathway triggered by an anticancer drug is important to predict the efficacy of a particular chemotherapeutic treatment including that agent. The HDIs are promising anticancer drugs as they selectively induce differentiation and cell death of transformed cells, and some of them are now under clinical trials for both solid and hematological tumors (3, 4, 6).

The selectivity of HDIs toward transformed cells as compared with untransformed normal cells has been confirmed by our work. We provide evidence that a single oncogenic lesion, such as EIA expression, renders IMR90 fibroblasts highly susceptible to cell death when grown in the presence of SAHA or TSA. We have also confirmed that mitochondria play a central role during HDI-mediated apoptotic response (5, 23, 24, 26). In addition, our data demonstrate that the initiator caspase-9 is critical for this cell death pathway. In IMR90-E1A and in MCF-7 cells, abrogation of caspase-9 activity suppressed apoptosis in response to TSA or SAHA and blocked processing of
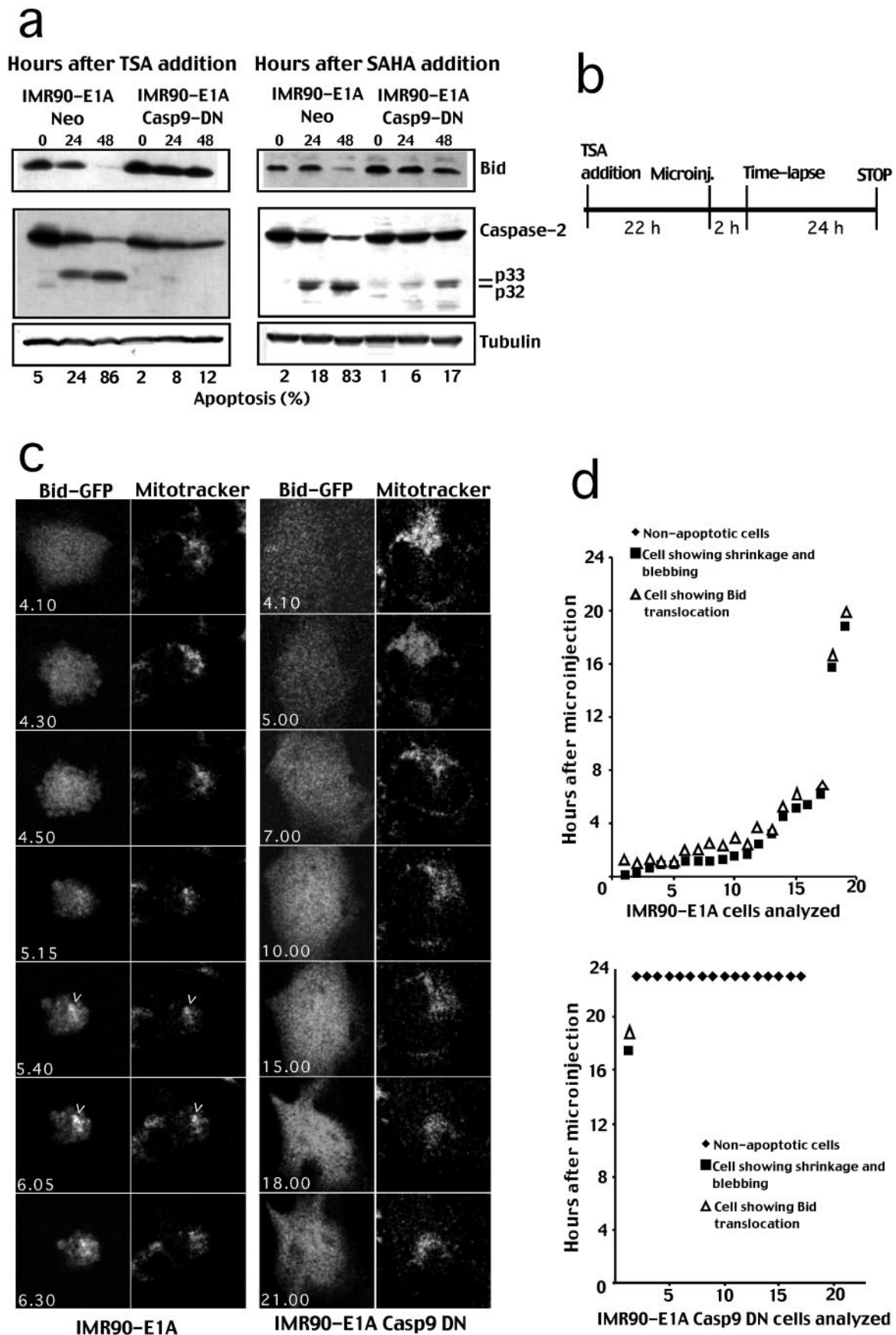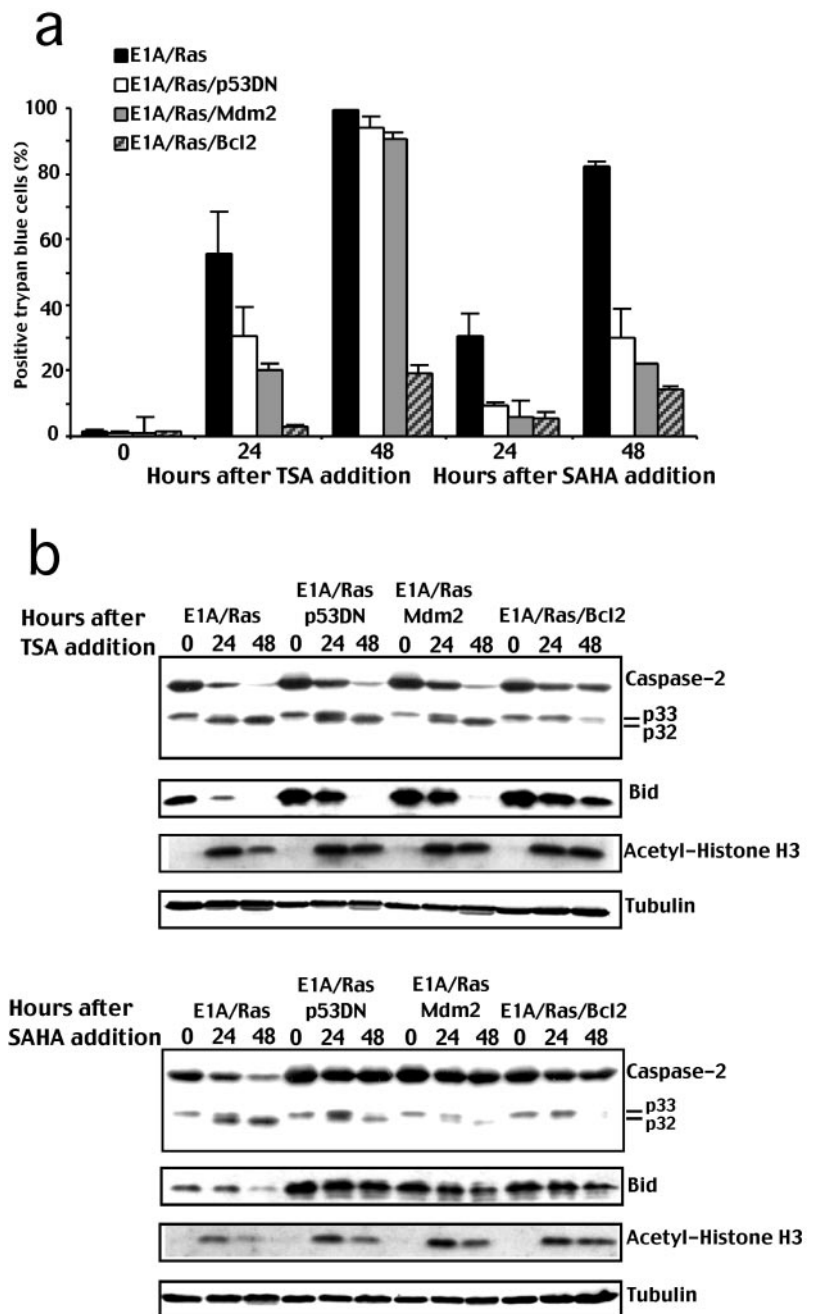
FIG. 5. **Bid processing and translocation to mitochondria require caspase-9 activity.** *a*, processing of Bid in IMR90-E1A/NEO and IMR90-EIA/Casp9-DN cells grown for the indicated time in the presence of TSA or SAHA. Equal amounts of IMR90-E1A/NEO and IMR90-EIA/Casp9-DN cell lysates were subjected to SDS-PAGE electrophoresis. Immunoblots were performed using the indicated antibodies. As shown in *b*, IMR90-E1A/NEO and IMR90-E1A/Casp9-DN cells 24 h after seeding were treated with TSA, and after 22 h, they were microinjected with pEGFP-N1-Bid (5 ng/μl). 2 h later, cells were subjected to time-lapse analysis for 24 h. *c*, time-lapse images of representative IMR90-E1A/NEO and

FIG. 6. **The apoptotic susceptibility to TSA and SAHA is dependent on p53.** As shown in *a*, BJ cells expressing E1A and Ha-RasV12, E1A Ha-RasV12 and MDM2, E1A Ha-RasV12 and p53DN, or E1A Ha-RasV12 and Bcl-2 were treated with TSA or SAHA for the indicated time points, and the appearance of apoptosis was scored with trypan blue staining as indicated under "Experimental Procedures." As shown in *b*, processing of caspase-2 and Bid in BJ cells expressing E1A and Ha-RasV12, E1A Ha-RasV12 and MDM2, E1A Ha-RasV12 and p53DN, or E1A Ha-RasV12 and Bcl-2 were treated with TSA or SAHA for the indicated time points. Equal amounts of cellular lysates were subjected to SDS-PAGE electrophoresis. Immunoblots were performed using the indicated antibodies.

PARP, caspase-2, -7, and -8.

TSA- and SAHA-induced processing of Bid and subsequent translocation to mitochondria were also dependent on caspase-9. These data suggest that Bid could play a role in the amplification loop rather than during the initial phase of the process in HDI-induced cell death. A late function of Bid is supported by the time-lapse analysis. Translocation of Bid to mitochondria was observed *in vivo* during TSA-induced cell death after 46.17 ($\pm$25.01) min from the appearance of the first signs of cell death (cell shrinkage and membrane blebbing). A previous study suggested that a caspase not efficiently inhibited by zVAD-fmk could be responsible for Bid cleavage in response to SAHA (23). The current study supports the notion

that this caspase is caspase-9 or a caspase regulated by caspase-9.

Our findings do not exclude a role for the initiator caspase-2 and -8 upstream of caspase-9 during HDI-induced cell death. We used proenzyme cleavage as marker of caspase-2 and -8 activation. However, regulative caspases might also be activated in the absence of proteolytic processing (44). Recent studies have showed that caspase-2 can be activated independently from proteolytic processing (45), and therefore, further investigations are needed to assess whether caspase-2 plays a role as regulator of the mitochondrial integrity (28, 46–48), upstream of caspase-9 during apoptosis induced by HDIs. Concerning caspase-8, a critical role of this initiator caspase during HDI-

---

IMR90-E1A/Casp9-DN cells treated with TSA and double-stained for Bid-GFP and mitochondria. *Arrowheads* indicate translocation of Bid-GFP to mitochondria. *d*, time-lapse sequences of IMR90-E1A/NEO and IMR90-E1A/Casp9-DN cells overexpressing Bid-GFP and treated with TSA. Each position along the *x* axis represents a single cell. *g* marks the appearance of the cell shrinkage and membrane blebbing; △ marks Bid translocation to mitochondria. Cells that at the end of the analysis did not showed apoptotic features were scored as non-apoptotic (*u*).
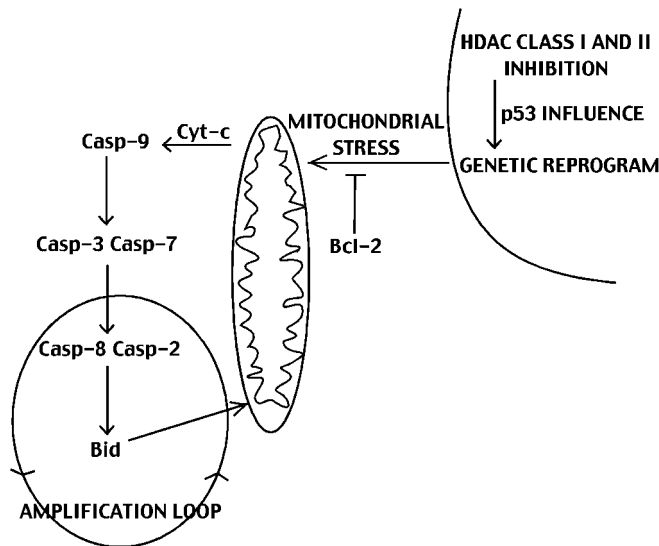
FIG. 7. **The critical elements of the apoptotic pathway triggered by HDIs TSA and SAHA.**

induced cell death should be excluded since it has been reported that its inhibition, through expression of the cowpox virus protein CrmA, did not affect SAHA-induced cell death (23).

We demonstrate that p53 is essential for an efficient apoptotic response to TSA and SAHA treatments. The role of p53 has been investigated by using primary human fibroblasts transformed with E1A and Ha-Ras-V12 where p53 was inactivated by ectopic expression MDM2 or p53DN mutant (42). Our data are in disagreement with a previous report, which suggested the existence of a p53-independent apoptotic pathway in response to SAHA (23). Indeed, although we find that p53 does affect the rate of HDI-induced cell death, prolonged treatments with these inhibitors can also induce a p53-independent response. It is thus likely that such a delayed p53-independent response was the one described previously (23).

Moreover, it has also been reported that conditional expression of p53 failed to modify the apoptotic response to SAHA in U937 cells (22). U937 cells do not express p73 (51), and it is known that the p53 family members p63 and p73 can modulate the p53 apoptotic response (49, 50). In fact, the combined loss of p63 and p73 results in the failure of cells containing functional p53 to undergo apoptosis in response to DNA damage (50). Therefore, the absence of p73 expression might account for the inability of these cells to mount a p53-dependent apoptosis in response to SAHA (22).

A differential behavior was noted for TSA- and SAHA-induced apoptosis relative to the rate of the dependence from p53. Cells lacking functional p53 were still resistant to cell death after long term treatments with SAHA (48 h), whereas apoptosis was induced in the same cells after long term treatments with TSA. One could postulate that since TSA is an inhibitor of HDACs at nanomolar range, whereas SAHA is efficient at micromolar range (3), this difference could mirror the potency of the two HDIs. In fact, we observed that histone H3 acetylation was more pronounced in cells treated with TSA.

Several models could be proposed for the relationship between HDIs and p53. It has been reported that TSA up-regulates p53 in endothelial cells (20), whereas HDAC1 can regulate p53 deacetylation, thereby reducing its transcriptional activity by targeting it for degradation (19, 21). Therefore, TSA and SAHA might activate p53, thus inducing the expression of p53 target genes involved in apoptosis. Array analysis of gene expression in our cellular system will allow us to better define the mechanism through which p53 regulates the apoptotic susceptibility to HDIs.

Interestingly, production of reactive oxygen species is crucial for cell death induced by SAHA (23, 25), and transcription of redox-related genes, formation of reactive oxigen species, and oxidative degradation of mitochondria components have been suggested to be critical for a p53-dependent apoptosis (43). As schematized in Fig. 7, we propose a model where the pattern of genes affected by TSA and SAHA can be influenced by the presence of p53 (directly or indirectly), and these genes can regulate the rate of cell death (apoptotic threshold).

In conclusion, our findings support the notion that HDI-induced apoptosis requires caspase-9 activation through the release of cytochrome *c* in a Bcl-2-dependent and p53-sensitive manner. This pathway seems to be common to other anticancer-treatments; however, one difference can be noted when TSA is compared with the DNA-damaging agent daunorubicin in cells lacking caspase-3 activity. Bid, PARP, caspase-2, and -8 processing can still occur in MCF-7/C3CI cells treated with TSA. This suggests that HDIs could effect the rate of caspase activation even when the amplification loop, which is largely based on caspase-3, is defective. Definition of the molecular events that permit overcoming the caspase-3 defect is an interesting question that requires further work.

REFERENCES

1. Narlikar, G. J., Fan, H. Y., and Kingston, R. E. (2002) *Cell* **108,** 475–487
2. Fischle, W., Kiermer, V., Dequiedt, F., and Verdin, E. (2001) *Biochem. Cell Biol.* **79,** 337–348
3. Melnick, A., and Licht, J. D. (2002) *Curr. Opin. Hematol.* **9,** 322–332
4. Marks, P. A., Rifkind, R. A., Richon, V. M., Breslow, R., Miller, T., and Kelly, W. K. (2001) *Nat. Rev. Cancer* **1,** 194–202
5. Medina, V., Edmonds, B., Young, G. P., James, R., Appleton, S., and Zalewski, P. D. (1997) *Cancer Res.* **57,** 3697–3707
6. Richon, V. M., Emiliani, S., Verdin, E., Webb, Y., Breslow, R., Rifkind, R. A., and Marks, P. A. (1998) *Proc. Natl. Acad. Sci. U. S. A.* **95,** 3003–3007
7. Wang, J., Saunthararajah, Y., Redner, R. L., and Liu, J. M. (1999) *Cancer Res.* **59,** 2766–2769
8. Butler, L. M., Agus, D. B., Scher, H. I., Higgins, B., Rose, A., Cordon-Cardo, C., Thaler, H. T., Rifkind, R. A., Marks, P. A., and Richon, V. M. (2000) *Cancer Res.* **60,** 5165–5170
9. Shi, Y. (2002) *Mol. Cell* **9,** 459–470
10. Cryns, V., and Yuan, J. (1998) *Genes Dev.* **12,** 1551–1570
11. Thornberry, N. A., and Lazebnik, Y. (1998) *Science* **281,** 1312–1316
12. Adrain, C., and Martin, S. J. (2001) *Trends Biochem. Sci.* **26,** 390–397
13. Wang, X. (2001) *Genes Dev.* **15,** 2922–2933
14. Nagata, S. (1999) *Annu. Rev. Genet.* **33,** 29–55
15. Bouillet, P., and Strasser, A. (2002) *J. Cell Sci.* **115,** 1567–1574
16. Soengas, M. S., Capodieci, P., Polsky, D., Mora, J., Esteller, M., Opitz-Araya, X., McCombie, R., Herman, J. G., Gerald, W. L., Lazebnik, Y. A., Cordon-Cardo, C., and Lowe, S. W. (2001) *Nature* **409,** 207–211
17. Liu, J. R., Opipari, A. W., Tan, L., Jiang, Y., Zhang, Y., Tang, H., and Nunez, G. (2002) *Cancer Res.* **62,** 924–931
18. Sambucetti, L. C., Fischer, D. D., Zabludoff, S., Kwon, P. O., Chamberlin, H., Trogani, N., Xu, H., and Cohen, D. (1999) *J. Biol. Chem.* **274,** 34940–34947
19. Juan, L. J., Shia, W. J., Chen, M. H., Yang, W. M., Seto, E., Lin, Y. S., and Wu, C. W. (2000) *J. Biol. Chem.* **275,** 20436–20443
20. Kim, M. S., Kwon, H. J., Lee, Y. M., Baek, J. H., Jang, J. E., Lee, S. W., Moon, E. J., Kim, H. S., Lee, S. K., Chung, H. Y., Kim, C. W., and Kim, K. W. (2001) *Nat. Med.* **7,** 437–443
21. Ito, A., Kawaguchi, Y., Lai, C. H., Kovacs, J. J., Higashimoto, Y., Appella, E., and Yao, T. P. (2002) *EMBO J.* **21,** 6236–6245
22. Vrana, J. A., Decker, R. H., Johnson, C. R., Wang, Z., Jarvis, W. D., Richon, V. M., Ehinger, M., Fisher, P. B., and Grant, S. (1999) *Oncogene* **18,** 7016–7025
23. Ruefli, A. A., Ausserlechner, M. J., Bernhard, D., Sutton, V. R., Tainton, K. M., Kofler, R., Smyth, M. J., and Johnstone, R. W. (2001) *Proc. Natl. Acad. Sci. U. S. A.* **98,** 10833–10838
24. Zhu, W. G., Lakshmanan, R. R., Beal, M. D., and Otterson, G. A. (2001) *Cancer Res.* **61,** 1327–1333
25. Butler, L. M., Zhou, X., Xu, W. S., Scher, H. I., Rifkind, R. A., Marks, P. A., and Richon, V. M. (2002) *Proc. Natl. Acad. Sci. U. S. A.* **99,** 11700–11705
26. Herold, C., Ganslmayer, M., Ocker, M., Hermann, M., Geerts, A., Hahn, E. G., and Schuppan, D. (2002) *J. Hepatol.* **36,** 233–240
27. Sawa, H., Murakami, H., Ohshima, Y., Sugino, T., Nakajyo, T., Kisanuki, T., Tamura, Y., Satone, A., Ide, W., Hashimoto, I., and Kamada, H. (2001) *Brain Tumor Pathol.* **18,** 109–114
28. Paroni, G., Henderson, C., Schneider, C., and Brancolini, C. (2002) *J. Biol. Chem.* **277,** 15147–15161

29. Scorrano, L., Petronilli, V., Colonna, R., Di Lisa, F., and Bernardi, P. (1999) *J. Biol. Chem.* **274,** 24657–24663
30. Hannon, G. J., Sun, P., Carnero, A., Xie, L. Y., Maestro, R., Conklin, D. S., and Beach, D. (1999) *Science* **283,** 1129–1130
31. Paroni, G., Henderson, C., Schneider, C., and Brancolini, C. (2001) *J. Biol. Chem.* **276,** 2190–21915
32. Talanian, R. V., Quinlan, C., Trautz, S., Hackett, M. C., Mankovich, J. A., Banach, D., Ghayur, T., Brady, K. D., and Wong, W. W. (1997) *J. Biol. Chem.* **272,** 9677–9682
33. Sanchez-Prieto, R., Rojas, J. M., Taya, Y., and Gutkind, J. S. (2000) *Cancer Res.* **60,** 2464–2472
34. Cuvillier, O., Mayhew, E., Janoff, A. S., and Spiegel, S. (1999) *Blood* **94,** 3583–3592
35. Germain, M., Affar, E. B., D'Amours, D., Dixit, V. M., Salvesen, G. S., and Poirier, G. G. (1999) *J. Biol. Chem.* **274,** 28379–28384
36. Faleiro, L., and Lazebnik, Y. (2000) *J. Cell Biol.* **151,** 951–960
37. Fearnhead, H. O., Rodriguez, J., Givek, E. E., Guo, W., Kobayashi, R., Hannon, G., and Lazebnik, Y. (1998) *Proc. Natl. Acad. Sci. U. S. A.* **95,** 13664–13669
38. Nahle, Z., Polakoff, J., Davuluri, R. V., McCurrach, M. E., Jacobson, M. D., Narita, M., Zhang, M. Q., Lazebnik, Y., Bar-Sagi, D., and Lowe, S. W. (2002) *Nat. Cell Biol.* **4,** 859–864
39. Vousden, K. H. (2000) *Cell* **103,** 691–694
40. de Stanchina, E., McCurrach, M. E., Zindy, F., Shieh, S. Y., Ferbeyre, G., Samuelson, A. V., Prives, C., Roussel, M. F., Sherr, C. J., and Lowe, S. W. (1998) *Genes Dev.* **12,** 2434–2442
41. Lowe, S. W. (1995) *Curr. Opin. Oncol.* **7,** 547–553
42. Seger, Y. R., Garcia-Cao, M., Piccinin, S., Cunsolo, C. L., Doglioni, C., Blasco, M. A., Hannon, G. J., and Maestro, R. (2002) *Cancer Cell* **2,** 401–413
43. Polyak, K., Xia, Y., Zweier, J. L., Kinzler, K. W., and Vogelstein, B. (1997) *Nature* **389,** 300–305
44. Stennicke, H. R., Deveraux, Q. L., Humke, E. W., Reed, J. C., Dixit, V. M., and Salvesen, G. S. (1999) *J. Biol. Chem.* **274,** 8359–8362
45. Read, S. H., Baliga, B. C., Ekert, P. G., Vaux, D. L., and Kumar, S. (2002) *J. Cell Biol.* **159,** 739–745
46. Lassus, P., Opitz-Araya, X., and Lazebnik, Y. (2002) *Science* **297,** 1352–1354
47. Robertson, J. D., Enoksson, M., Suomela, M., Zhivotovsky, B., and Orrenius, S. (2002) *J. Biol. Chem.* **277,** 29803–29809
48. Guo, Y., Srinivasula, S. M., Druilhe, A., Fernandes-Alnemri, T., and Alnemri, E. S. (2002) *J. Biol. Chem.* **277,** 13430–13437
49. Zacchi, P., Gostissa, M., Uchida, T., Salvagno, C., Avolio, F., Volinia, S., Ronai, Z., Blandino, G., Schneider, C., and Del Sal G. (2002) *Nature* **419,** 853–857
50. Flores, E. R., Tsai, K. Y., Crowley, D., Sengupta, S., Yang, A., McKeon, F., and Jacks, T. (2002) *Nature* **416,** 560–564
51. Stiewe, T., and Putzer, B. M. (2000) *Nat. Genet.* **26,** 464–469

Role of Caspases, Bid, and p53 in the Apoptotic Response Triggered by Histone Deacetylase Inhibitors Trichostatin-A (TSA) and Suberoylanilide Hydroxamic Acid (SAHA)

Clare Henderson, Michela Mizzau, Gabriela Paroni, Roberta Maestro, Claudio Schneider and Claudio Brancolini

Access the most updated version of this article at doi: 10.1074/jbc.M213093200

Alerts:
- When this article is cited
- When a correction for this article is posted

Click here to choose from all of JBC's e-mail alerts

This article cites 51 references, 30 of which can be accessed free at
http://www.jbc.org/content/278/14/12579.full.html#ref-list-1